Electrocatalytic Reduction of Nitrite and Nitric Oxide to Ammonia with Iron-Substituted Polyoxotungstates†

James E. Toth and Fred C. Anson*

Contribution from the Arthur Amos Noyes Laboratories, Division of Chemistry and Chemical Engineering, California Institute of Technology, Pasadena, California 91125.
Received August 15, 1988

Abstract: Heteropolytungstates in which one of the positions normally occupied by a tungsten cation is occupied instead by an iron cation are shown to be catalysts for the electroreduction of nitrite to ammonia. The lacunary derivatives in which the empty tungsten site is unoccupied show no catalytic activity. The catalytic mechanism involves the intermediate formation of a nitrosyl complex of the Fe(II) form of the catalyst. The pH dependence of the rate of formation of the nitrosyl complex shows that nitrous acid is the reactive form of nitrite between pH 2 and 8. The catalyzed reduction does not produce hydroxylamine as an intermediate and appears to depend upon the ability of the multiply reduced heteropolytungstates to deliver electrons to the NO group bound to the iron center in a concerted, multiple-electron step. The iron-substituted heteropolytungstates are not degraded by repeated cycling between their oxidized and reduced states. A particularly valuable feature of the heteropolytungstate is the ease with which the formal potentials of the several redox couples they exhibit may be shifted by changing the identity of the central heteroatom. Exploitation of this feature provides diagnostic information that can be decisive in establishing the mechanism of electrocatalytic processes.

The efficient electrochemical catalysis of multiple-electron processes is an area of continuing interest. The stability of traditional, transition-metal complexes that are frequently employed as catalysts is often limited by degradation of the organic ligands that surround the active sites of the catalysts. These organic ligands are often susceptible to oxidation by reactive, radical intermediates that must be formed along the reaction pathway if the catalyst is capable of transferring only single electrons to the substrate. Approaches that suggest themselves as means to minimize these problems include the design of electrocatalysts that are capable of delivering multiple electrons to a substrate in order to avoid radical intermediates. In addition, catalysts with ligands that are more inert toward oxidizing environments could prove useful. In the hope of developing more robust catalysts we have begun the study of the electrochemical activity of a series of transition-metal-substituted heteropolytungstates.[1] These compounds consist of a transition metal coordinated to a totally inorganic tungsten–oxo framework that is inert to typical ligand oxidation reactions. It is possible to reduce these complexes reversibly by up to five electrons, which could facilitate the catalysis of multiple-electron processes. Thus, these compounds seemed capable of meeting both of the design criteria mentioned above.

The iron-substituted polyoxoanions that are the subject of this report are derived from the well-known Keggin ions that have the general formula $XW_{12}O_{40}^{m-}$, where X is a tetrahedrally coordinated heteroatom such as silicon that is located in the center of a tungsten–oxo cage.[2] In 1966, Baker and co-workers reported that it was possible to substitute various transition metals for one of the tungsten cations and its terminal oxo group located on the periphery of the anion.[3] It has since been shown that the tungsten–oxo cage acts as a pentadentate, homoleptic ligand for the incorporated transition metal, with five bridging oxide ions available for coordination.[4] The incorporated transition metal typically resides in a pseudooctahedral environment with one coordination site occupied by a labile water molecule, which can be substituted with other ligands.[5,6] Although the parent $XW_{12}O_{40}^{m-}$ compounds have been the subject of numerous electrochemical studies,[7-9] the electrocatalytic activity of the transition-metal-substituted analogues has yet to be examined, in spite of the fact that the open coordination site of the incorporated transition metal could provide a pathway for inner-sphere electron transfer which is probably unavailable to the parent $XW_{12}O_{40}^{m-}$ compounds. We were interested in determining if these compounds would exhibit the reactivity of traditional transition-metal catalysts combined with the high stability of the polyoxoanions.

The transition-metal-substituted heteropolytungstates are also attractive because of a very significant diagnostic advantage they offer in examining the mechanisms of electron-transfer reactions in which they participate: The central heteroatom that is embedded in the center of the multinuclear anion is inaccessible to species in solution and therefore cannot participate directly in reactions that occur at the periphery of the ion. However, changes in the identity of this heteroatom produce systematic changes in the redox potentials of both the transition-metal center and the tungsten–oxo cage.[1,10] This feature can be exploited to determine the likely site of electrocatalytic activity in the multinuclear anions by noting how the potentials where catalyzed electrode reactions proceed are affected by changes in the centeral heteroatom. The diagnostic value of this tactic is exemplified in the present study.

The electroreduction of nitrite ion to ammonia requires a large overpotential at most electrode surfaces but the reduction can be catalyzed in aqueous solution by various transition-metal complexes including iron chelates,[11] iron porphyrins,[12] and nickel and

† Contribution No. 7833.

(1) Toth, J. E.; Anson, F. C. *J. Electroanal. Chem.* **1988**, *256*, 361.
(2) Pope, M. T. *Heteropoly and Isopoly Oxometallates*; Springer-Verlag: Berlin, 1983; p 23.
(3) Baker, L. C. W.; Baker, V. E. S.; Eriks, K.; Pope, M. T.; Shibata, M.; Rollins, O. W.; Fang, J. H.; Koh, L. L. *J. Am. Chem. Soc.* **1966**, *88*, 2329.
(4) Reference 2, p 93.
(5) (a) Zonnevijlle, F.; Tourné, C. M.; Tourné, F. T. *Inorg. Chem.* **1983**, *22*, 1198. (b) Zonnevijlle, F.; Tourné, C. M.; Tourné, F. T. *Inorg. Chem.* **1982**, *21*, 2751.
(6) Weakley, T. J. R. *J. Chem. Soc., Dalton Trans.* **1973**, 341.
(7) Pope, M. T.; Varga, G. M. *Inorg. Chem.* **1966**, *5*, 1249.
(8) McEvoy, A. J.; Gratzel, M. *J. Electroanal. Chem.* **1986**, *209*, 391.
(9) (a) Keita, B.; Nadjo, L. *J. Electroanal. Chem.* **1988**, *247*, 157. (b) Keita, B.; Nadjo, L.; Saveant, J. M. *J. Electroanal. Chem.* **1988**, *243*, 105. (c) Keita, B.; Nadjo, L. *J. Electroanal. Chem.* **1988**, *243*, 87. (d) Keita, B.; Nadjo, L. *J. Electroanal. Chem.* **1988**, *240*, 325. (e) Keita, B.; Nadjo, L.; Haeussler, J. P. *J. Electroanal. Chem.* **1987**, *230*, 85. (f) Keita, B.; Nadjo, L. *J. Electroanal. Chem.* **1987**, *227*, 265. (g) Keita, B.; Nadjo, L. *J. Electroanal. Chem.* **1986**, *199*, 229. (h) Keita, B.; Lucas, T.; Nadjo, L. *J. Electroanal. Chem.* **1986**, *208*, 343. (i) Keita, B.; Nadjo, L. *J. Electroanal. Chem.* **1985**, *191*, 441. (j) Keita, B.; Nadjo, L. *J. Electroanal. Chem.* **1987**, *230*, 267. (k) Keita, B.; Nadjo, L. *J. Electroanal. Chem.* **1987**, *227*, 77. (l) Keita, B.; Nadjo, L. *J. Electroanal. Chem.* **1987**, *219*, 355. (m) Keita, B.; Nadjo, L. *J. Electroanal. Chem.* **1987**, *217*, 287.
(10) Tourné, C. M.; Tourné, F. T.; Malik, S. A.; Weakley, T. J. R. *Inorg. Nucl. Chem.* **1970**, *32*, 3875.
(11) Ogura, K.; Ishikawa, H. *J. Chem. Soc., Faraday Trans. 1* **1984**, *80*, 2243.
(12) (a) Barley, M. H.; Takeuchi, K. J.; Meyer, T. J. *J. Am. Chem. Soc.* **1986**, *108*, 5876. (b) Barley, M. M.; Rhodes, M. R.; Meyer, T. J. *Inorg. Chem.* **1987**, *26*, 1746.

0002-7863/89/1511-2444$01.50/0

cobalt cyclams.[13] However, with all of these catalysts, hydroxylamine is either the major product or a significant side product, and the reduction is believed to occur via a series of one-electron steps. This proved to be the case even when *N*-methylpyridinium groups were covalently attached to an iron porphyrin in an attempt to obtain a catalyst that would be capable of delivering multiple electrons.[12b] By contrast, the iron-substituted heteropolytungstates examined in this study appear to accomplish a multiple-electron reduction of nitrite and nitric oxide to ammonia and other products without the formation of hydroxylamine. In addition, controlled-potential electrolyses involving a large number of catalyst turnovers showed these anions to have excellent long-term durability.

Experimental Section

Materials. Unsubstituted and iron-substituted heteropolytungstates were prepared as the α isomers and purified as described previously.[5a] Gaseous nitric oxide was passed through a short column of KOH prior to use. Deionized water was further purified by passage through a purification train (Barnsted Nanopure). Prepurified argon was deoxygenated by passage through acidic solutions of V(II). All other chemicals were reagent grade and used as received. Buffer solutions (0.1 M) were prepared by partial neutralization of the following acids: HSO_4^- (pH 2); Cl_3COOH (pH 2.5–3); CH_3COOH (pH 3.5–6.0); morpholinoethanesulfonic acid, MES (pH 6–7); (hydroxyethyl)piperazinesulfonic acid, HEPES (pH 7–8).

Solutions of the reduced (Fe(II)) forms of the heteropolytungstates were prepared by controlled-potential electrolysis of solutions of the Fe(III) forms and were handled under argon using standard Schlenk line techniques. Solutions of the air-sensitive nitrosyl complexes could be obtained either by exhaustive controlled-potential electrolysis of equimolar amounts of the Fe(III)-substituted ions and nitrite ion at potentials just negative of the peak potential of the Fe^{III}/Fe^{II} couples or by saturation of Fe(II) solutions with NO gas for ca. 3 min. Solutions prepared by either technique displayed identical spectra and chemical properties. Tetra-*n*-butylammonium salts of the nitrosyl complexes were isolated by precipitation with tetra-*n*-butylammonium bromide at pH $\leq$ 4 and were handled under nitrogen in a drybox. KBr pellets containing the air-sensitive nitrosyl complexes were prepared in a drybox and sandwiched on both sides with pure KBr to limit oxygen exposure while the spectra were being recorded.

Apparatus and Procedures. Electrochemical measurements were conducted under argon in conventional two- and three-compartment cells with a glassy carbon working electrode, platinum wire counter electrode and a sodium chloride saturated calomel reference electrode (SSCE). Formal potentials for reversible couples were taken as the average of anodic and cathodic peak potentials. The working electrode (0.20 cm^2) was polished with 0.3-μm alumina and washed with purified water before use. A combination of Princeton Applied Research instrumentation was used to record cyclic voltammograms and to conduct controlled-potential electrolyses at stirred mercury pool electrodes. During unusually extensive electrolyses small quantities of deoxygenated acetic acid were injected into the cell if the pH of the buffer solutions began to change.

UV–vis spectra were recorded on a Hewlett-Packard Model 8450A spectrophotometer. Kinetic runs were performed on this spectrophotometer or with a Durham Model D110 stopped-flow spectrophotometer equipped with a Tektronix Model 5223 storage oscilloscope. Sodium nitrite and $H_2OFe^{II}XW_{11}O_{39}^{(n+1)-}$ solutions were prepared fresh daily. Standardization of the nitrite solutions with permanganate[15] revealed that there was no decomposition over the course of several hours. All kinetic runs were carried out at constant ionic strength (0.1 M) and under pseudo-first-order conditions with nitrite present in at least a tenfold excess. The extent of reaction was typically followed at two wavelengths: near 460 nm, where the nitrosyl complexes have maxima, and near 700 nm, where the $Fe^{II}XW_{11}O_{39}^{(n+1)-}$ complexes absorb strongly. Pseudo-first-order rate constants were obtained from plots of ln $(A - A_\infty)$ vs time.

Electrolysis solutions were analyzed for ammonia as ammonium cation by ion chromatography (Dionex Model 2020i). Hydroxylamine was determined as the indoxine after reaction with 8-quinolinol in solutions freed of any gaseous, nitrogen-based products (i.e., NO, N_2, N_2O) by purging with air for 10 min and adjusting the solution pH to 7.[16] The concentration of indoxine was measured spectrophotometrically at pH 6.8 at λ = 706 nm; $\epsilon = 4.3 \times 10^3$.[16] Blank runs revealed that ammonium, nitrite, nitrate, and acetate ions as well as the various iron-substituted heteropolytungstates did not interfere with the procedure. As a check, known amounts of hydroxylammonium chloride were added to electrolysis solutions and the analysis procedure was repeated. In no case was any interference observed by any of the species present in solution after electrolyses.

Infrared spectra of the nitrosyl complexes were recorded on a Beckman Instruments Model 4240 IR spectrometer.

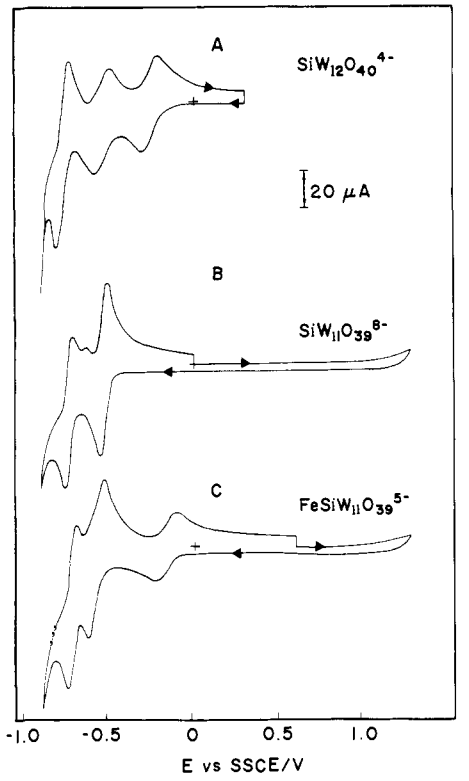

Figure 1. Cyclic voltammetry of 1 mM solutions of silicon polytungstate anions at a glassy carbon electrode: (A) $SiW_{12}O_{40}^{4-}$; (B) $SiW_{11}O_{39}^{8-}$; (C) $Fe^{III}SiW_{11}O_{39}^{5-}$. Supporting electrolyte: 0.1 M $NaClO_4$ + 0.01 M $HClO_4$. Scan rate = 50 mV s^{-1}. Reduction currents were recorded downward.

Results

Electrochemical Response of the Heteropolyanions. Four iron-substituted heteropolytungstates were examined in this study: $H_2OFe^{III}XW_{11}O_{39}^{n-}$ (X = Si or Ge, n = 5; X = As or P, n = 4). Their basic electrochemistry in the absence of reducible substrates has been described recently.[1] $H_2OFeSiW_{11}O_{39}^{5-}$, $H_2OFeGeW_{11}O_{39}^{5-}$, and $H_2OFePW_{11}O_{39}^{4-}$ are stable between pH 2 and 8. $H_2OFeAsW_{11}O_{39}^{4-}$ is stable between pH 2 and 6. The three cyclic voltammograms in Figure 1 contrast the behavior of one of the unsubstituted parent anions, $SiW_{12}O_{40}^{4-}$, the lacunary anion obtained by removal of one tungsten cation and its terminally bound oxo group, $SiW_{11}O_{39}^{8-}$, and the iron-substituted anion, $H_2OFeSiW_{11}O_{39}^{5-}$. The voltammogram for $SiW_{12}O_{40}^{4-}$ in the potential range of interest consists of two, reversible, one-electron waves followed by a reversible two-electron wave[7-9] (Figure 1A). Removal of the tungsten–oxo group to produce the lacunary anion leads to a voltammogram with two, reversible, two-electron waves (Figure 1B). When an iron(III) center is substituted into the vacant site of the lacunary ion, a new, reversible, one-electron wave appears at a more positive potential and the positions of the pair of two-electron waves of the lacunary ion are shifted slightly. The new, one-electron wave has been assigned to the reduction of the bound iron(III) to iron(II),[1,5] and the two-electron waves at more

(13) Taniguchi, I.; Nakashima, N.; Matsushita, K.; Yasukouchi, K. *J. Electroanal. Chem.* **1987**, *224*, 199.

(14) (a) Murphy, W. R., Jr.; Takeuchi, K.; Barley, M. H. *Inorg. Chem.* **1986**, *25*, 1041. (b) Murphy, W. R., Jr.; Takeuchi, K. J.; Meyer, T. J. *J. Am. Chem. Soc.* **1982**, *104*, 5817. (c) Barley, M. H.; Takeuchi, K. J.; Murphy, W. R., Jr.; Meyer, T. J. *J. Chem. Soc., Chem. Commun.* **1985**, 507.

(15) Vogel, A. *A Textbook of Quantitative Inorganic Analysis*, 4th ed.; Longman House: London, 1983; p 356.

(16) Snell, L. T.; Snell, F. D. *Colorimetric Methods of Analysis*, 3rd ed.; Van Nostrand and Co.: New York, 1967; Vol. IVA, p 174.

Table I. Correlation of Formal Potentials for $Fe^{III}XW_{11}O_{39}^{n-}/Fe^{II}XW_{11}O_{39}^{(n+1)-}$ Couples with Their Spectral and Kinetic Properties

X	E^f,[a] mV vs SCCE	ν,[b] cm^{-1}	k_{obsd},[c] $M^{-1}\ s^{-1}$
Si	−210	1710	1.3 ± 0.1
Ge	−138	1720	1.0 ± 0.1
P	−20	1730	0.6 ± 0.1
As	58	1750	0.4 ± 0.1

[a] Formal potential measured at pH 5 and 0.1 M ionic strength. [b] Peak in infrared band assigned to NO stretch in tetra-*n*-butylammonium salt of $ONFe^{II}XW_{11}O_{39}^{(n+1)-}$. [c] Observed second-order rate constant for the formation of the nitrosyl complex evaluated at pH 5. The indicated uncertainties are standard deviations for a series of runs at different concentrations of NO_2^-.

negative potentials have been assigned to the reduction of tungsten centers in the polyoxometalate framework. Controlled-potential electrolysis of the iron-substituted anion at ca. −350 mV consumes one electron and produces very darkly colored solutions that exhibit an extremely broad and featureless absorption that spans essentially the entire visible portion of the spectrum (ϵ = 200 $M^{-1}\ cm^{-1}$ at λ = 500 nm). These reduced solutions are air-sensitive but appear stable indefinitely under anaerobic conditions. The formal potentials of the iron-based waves depend upon the identity of the central heteroatom (see Table I) as well as the pH and ionic strength.[1]

Formation of Iron(II) Nitrosyl Complexes. Addition of an equimolar quantity of $NaNO_2$ to a solution of $H_2OFe^{III}SiW_{11}O_{39}^{5-}$ produces no changes in the spectrum of the solution indicative of a reaction between the two anions. However, there are significant changes in the voltammetry of the mixed solution as shown in Figure 2. At pH 2 the cathodic peak current of the first, iron-based wave is enhanced while its anodic counterpart is greatly diminished and the two two-electron waves at more negative potentials are also greatly enhanced (Figure 2A). It seems clear that the reduced forms of the heteropolyanion react with the added nitrite. As the pH increases, the enhancement of the current at potentials corresponding to the Fe^{III}/Fe^{II} couple decreases. For example, at pH 5 the addition of nitrite is virtually without effect on the Fe^{III}/Fe^{II} response (Figure 2B). However, the two-electron reduction waves of the $H_2OFe^{II}SiW_{11}O_{39}^{6-}$ anion that appear at more negative potentials are still significantly enhanced by the addition of nitrite (Figure 2C) so that at pH 5 the reduction of nitrite appears to be catalyzed by the multiply, but not the singly reduced forms of the iron-substituted heteropolytungstate. The presence of the iron center is essential for the catalysis because nitrite is without effect on the voltammetry of the lacunary derivative, $SiW_{11}O_{39}^{8-}$, despite the fact that this anion exhibits voltammetric responses at potentials similar to, or even more negative than, those of the $H_2OFe^{III}SiW_{11}O_{39}^{5-}$ anion (Figure 2D). Although the catalytic rate decreases significantly as the pH is increased, most of the experiments were conducted at pH 4 or above in order to avoid complications associated with the possible disproportionation of HNO_2.[17]

Controlled-potential reduction of equimolar mixtures of NO_2^- and $H_2OFe^{III}SiW_{11}O_{39}^{5-}$ at −400 mV in solutions buffered at pH 4 consumes 2 electrons per heteropolyanion and yields a pale red solution that contains an Fe^{II}–NO adduct (vide infra). The iron-substituted heteropolytungstates with Ge, P, and As as heteroatoms behave similarly when the iron center is reduced in the presence of nitrite.

The coulometry at a reduction potential of −400 mV is consistent with the following reaction sequence

$$2H_2OFe^{III}SiW_{11}O_{39}^{5-} + 2e^- \rightarrow 2H_2OFe^{II}SiW_{11}O_{39}^{6-} \quad (1)$$

$$2H_2OFe^{II}SiW_{11}O_{39}^{5-} + NO_2^- + 2H^+ \rightarrow ONFe^{II}SiW_{11}O_{39}^{6-} + H_2OFe^{III}SiW_{11}O_{39}^{5-} + 2H_2O \quad (2)$$

(17) Jolly, W. L. *The Inorganic Chemistry of Nitrogen*; W. A. Benjamin: New York, 1964; p 78.

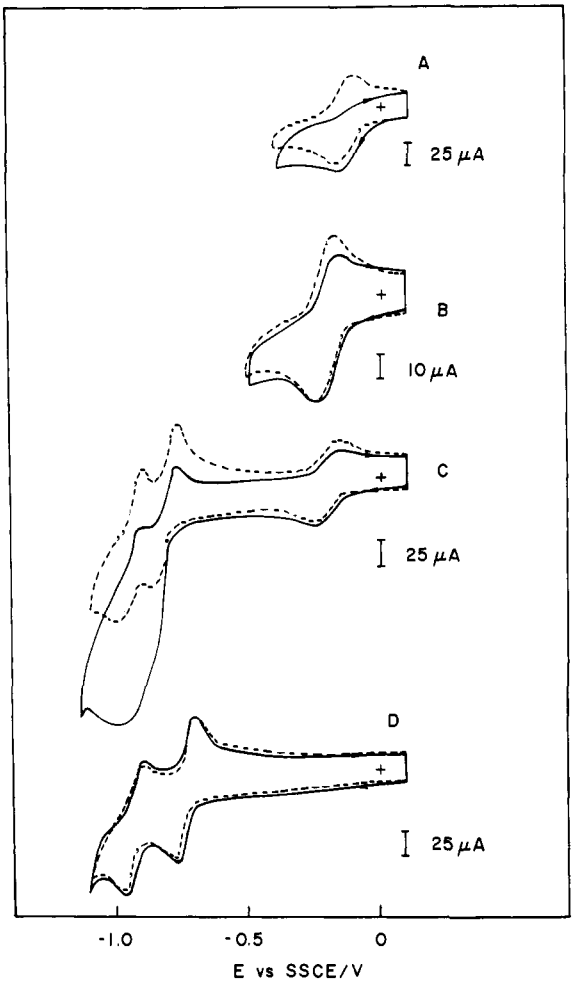

Figure 2. Cyclic voltammograms of 1 mM solutions of $Fe^{III}SiW_{11}O_{39}^{5-}$ (A–C) and $SiW_{11}O_{39}^{8-}$ (D) before (---) and after (—) addition of 1 mM NO_2^-. (A) Scan restricted to the Fe^{III}/Fe^{II} couple; supporting electrolyte: 0.1 M $NaHSO_4$–Na_2SO_4 at pH 2. (B) As in A; supporting electrolyte: 0.1 M CH_3COONa–CH_3COOH at pH 5. (C) The entire wave; supporting electrolyte as in B. (D) The lacunary anion; supporting electrolyte as in B. Scan rate = 50 mV s^{-1}. Reduction currents were recorded downward.

in which one Fe(II) center reduces the NO_2^- to NO, which coordinates to the second Fe(II) center in the labile site normally occupied by a water molecule.

The absorption spectra of the reduced solutions have a maximum that varies between 460 and 470 nm depending on the identity of the central heteroatom. The spectra resemble that of the well-characterized ONFe(edta) complex (edta = ethylenediaminetetraacetate) for which λ_{max} = 440 nm.[18] Infrared spectra of the insoluble tetra-*n*-butylammonium salts of the complexes, prepared by reduction of the Fe(III) center in the presence of nitrite, were measured in KBr disks protected from atmospheric oxygen (see Experimental Section). A prominent band assignable to a NO stretching mode[19] was observed near 1750 cm^{-1}. The exact position of the band varied with the formal potential of the Fe^{III}/Fe^{II} couple in a manner that is consistent with this assignment (Table I); i.e., the more strongly reducing complexes exhibited the weaker nitrogen–oxygen bonds expected from back-donation into π^* orbitals of the coordinated NO.

Complexes with spectra identical with those prepared electrochemically by reduction of $H_2OFe^{III}XW_{11}O_{39}^{n-}$ in the presence of NO_2^- can also be prepared by direct reaction between gaseous NO and the reduced $H_2OFe^{II}XW_{11}O_{39}^{(n+1)-}$ anions. The pale red

(18) Ogura, K.; Ozeki, T. *Electrochim. Acta* **1981**, *26*, 877. Ogura, K.; Watanabe, M. *Electrochim. Acta* **1982**, *27*, 111. Ogura, K.; Ishikawa, M. *Electrochim. Acta* **1983**, *28*, 167.

(19) Gans, P.; Sabatini, A.; Sacconi, L. *Coord. Chem. Rev.* **1966**, *1*, 187.

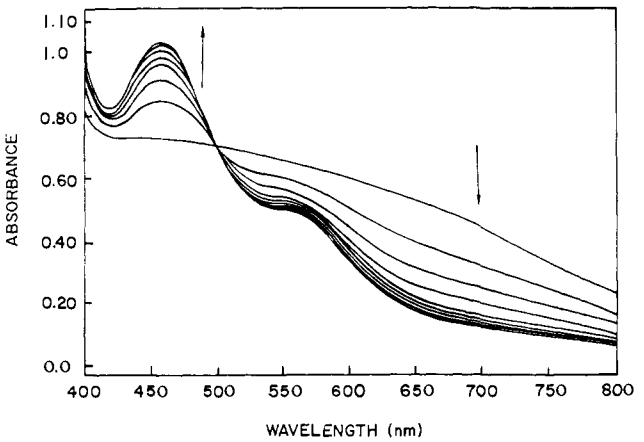

Figure 3. Absorption spectra of a mixture of $Fe^{II}GeW_{11}O_{39}^{6-}$ and NO_2^- at pH = 7. Spectra were recorded at 8-min intervals. Initial concentrations: $Fe^{II}GeW_{11}O_{39}^{6-}$, ca. 2 mM; NO_2^-, 40 mM.

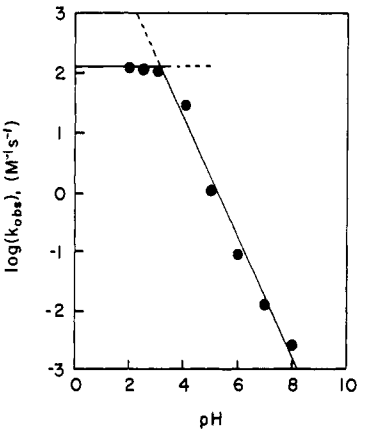

Figure 4. pH dependence of the second-order rate constants for the reaction of $Fe^{II}GeW_{11}O_{39}^{6-}$ with NO_2^- as obtained from spectral data such as those in Figure 3. k_{obsd} is the measured pseudo-first-order rate constant divided by the analytical concentration of nitrite.

NO adduct prepared in this way is converted to the original $H_2OFe^{II}XW_{11}O_{39}^{(n+1)-}$ anion when NO is removed from the solution by argon bubbling for ca. 15 min. Such reversible formation of a nitrosyl adduct has also been reported for Fe^{II}(edta) and related complexes.[18] Addition of NO to solutions of the unreduced Fe(III) forms of the heteropolytungstates produced no evidence of reaction.

Kinetics of Formation of Nitrosyl Adducts. The reaction between $H_2OFe^{II}XW_{11}O_{39}^{(n+1)-}$ anions and nitrite to form the nitrosyl complex proceeds cleanly and at an easily measured rate. The large spectral changes associated with the reaction, shown in Figure 3 for the representative $H_2OFe^{II}GeW_{11}O_{39}^{6-}$ anion at pH = 7, facilitated the measurement of reaction rates spectrophotometrically. The reaction rate is first order with respect to total nitrite and to the concentration of the heteropolytungstate anion. The rate is also pH dependent as shown in Figure 4. The observed second-order rate constant, k_{obsd}, is proportional to the proton concentration between pH 4 and 8 (the slope of a linear least-squares fit to the data points between pH 4 and 8 is 0.998) and becomes essentially independent of pH between pH 4 and 2. The intersection of the horizontal line in Figure 4 with the least-squares line drawn through the measured values of k_{obsd} at pH > 4 occurs at pH = 3.3, which is the pK_a of HNO_2. Thus, the kinetic data point to HNO_2 as the reactive form of nitrite in the reaction being monitored.[20] The rate constants obtained for the four heteropolyanions are listed in Table I. The particular reactions whose rates we believe are governed by these rate constants will be specified in the Discussion.

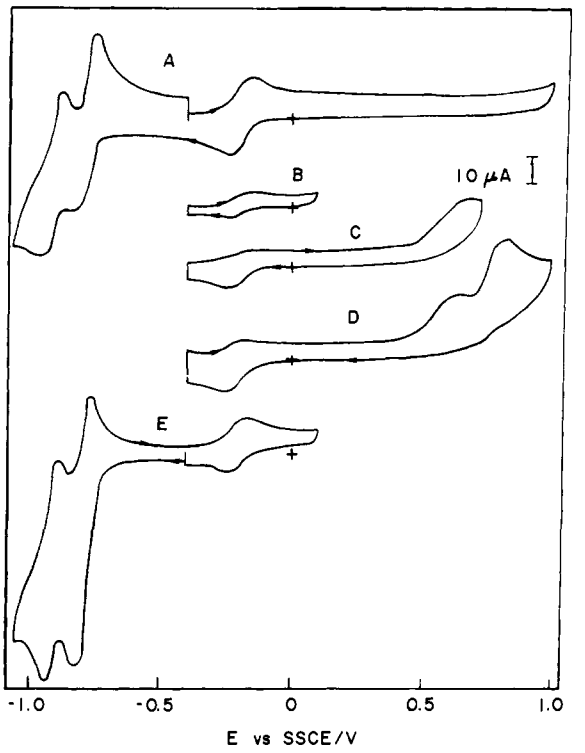

Figure 5. Cyclic voltammetry of 1 mM $Fe^{II}SiW_{11}O_{39}^{6-}$ before (A) and after (B–E) formation of $ONFe^{II}SiW_{11}O_{39}^{6-}$ by bubbling with NO followed by rapid purging with argon. Supporting electrolyte: 0.1 M CH_3COONa–CH_3COOH at pH 4.5. Scan rate = 50 mV s^{-1}. All scans commence at −400 mV. The initial scan direction was to more positive potentials in curves A–D and to more negative potentials in curve E. Reduction currents were recorded downward.

Electrochemistry of $ONFe^{II}XW_{11}O_{39}^{(n+1)-}$. To avoid complications from the electroactivity of the NO and NO_2^- ligands themselves, it is convenient to prepare solutions of $ONFe^{II}XW_{11}O_{39}^{(n+1)-}$ complexes by reacting NO with $H_2OFe^{II}XW_{11}O_{39}^{(n+1)-}$ and quickly removing the excess NO by bubbling argon through the solution for a few minutes and then over the surface of the solution. The resulting complexes appear spectrally identical with those prepared in the presence of excesses of NO_2^- or NO, and their dissociative decompositions proceed sufficiently slowly to allow their electrochemistry to be examined in the absence of significant free ligand.

Curve A in Figure 5 is a cyclic voltammogram for a solution of $H_2OFe^{II}SiW_{11}O_{39}^{6-}$ prepared by electrolysis of the Fe(III) derivative. The assignment of the three waves has been discussed in connection with Figure 1. The voltammogram in curve B was obtained after the solution was saturated with NO for 3 min followed by the rapid removal of excess NO as described above. The response arising from the Fe^{III}/Fe^{II} couple in the heteropolyanion is much diminished because NO is coordinated to most of the Fe centers, which produces a large positive shift in their oxidation potential, as expected for significant back-donation into the low-lying π^* orbitals of the NO. Extension of the potential scan to more positive potentials revealed two new, irreversible anodic peaks between 700 and 1000 mV (curve D). The first new wave consumed more than one electron per iron center and seems likely to represent a composite oxidation of Fe(II) to Fe(III) and of the coordinated NO to NO_2^-. During the return scan the presence of the original Fe(III) center was revealed by the increase in the cathodic peak current at −150 mV. The second new anodic peak in curve D appeared at the same position where the oxidation of NO_2^- to NO_3^- was observed in separate experiments in the same

(20) In a recent study of the reaction of HNO_2/NO_2^- with Fe^{II}(edta), NO^+ was suggested as the reactive form of N(III) at low pH.[21] This possibility could be ruled out in the present experiments by the pH independence of the reaction rate at pH < 4.

(21) Zang, V.; Kotowski, M.; Van Eldik, R. *Inorg. Chem.* **1988**, *27*, 3279.

supporting electrolyte in the absence of any heteropolyanion.

Repetition of the experiment of Figure 5D with the germanium complex, ON $Fe^{II}GeW_{11}O_{39}^{6-}$, produced a positive shift of 100 mV in the first new anodic peak. The same positive shift also occurs in the formal potential of the Fe^{III}/Fe^{II} couple in the corresponding parent complex, $H_2OFe^{III}GeW_{11}O_{39}^{5-}$ (Table I). The second new anodic peak in solutions of the $ONFe^{II}GeW_{11}O_{39}^{6-}$ complex appeared at the same position as the second new anodic peak of the $ONFe^{II}SiW_{11}O_{39}^{6-}$ complex, as expected for a wave arising from the oxidation of uncoordinated NO_2^- to NO_3^-.

Experiments with the corresponding As and P heteropolyanions produced similar results except that a further positive shift in the first new anodic peak caused the two anodic peaks to merge. Cycling the potential over the merged peaks produced the same increase in the Fe^{III}/Fe^{II} response at −150 mV that occurred with the other complexes.

Examination of the voltammetry of the nitrosyl complexes in the vicinity of the waves corresponding to the reduction of the tungsten cage in the parent, iron-substituted heteropolyanion revealed large enhancements in the reduction currents (curve E, Figure 5). Scanning the potential over the enhanced cathodic peaks led to the reappearance of the Fe^{III}/Fe^{II} response at −150 mV on the return scan, indicating that the unsubstituted parent complex, $H_2OFe^{II}SiW_{11}O_{39}^{6-}$, is generated during the cathodic cycle. Changing the central heteroatom of the heteropolyanion produced shifts in the reduction waves for the nitrosyl complexes similar to those observed for the tungsten-based waves of the parent complexes.

Controlled-Potential Electrolytic Reductions. Electrolysis of solutions containing mixtures of $H_2OFe^{III}XW_{11}O_{39}^{n-}$ and NO_2^- at stirred, mercury pool electrodes maintained at potentials negative of the second, two-electron, cathodic wave (e.g., −900 mV) proceeded in two stages. Early in the electrolysis the pale red color of the nitrosyl complex developed just as it did when the electrolysis was conducted at potentials just negative of the first, one-electron wave (vide supra). However, as the electrolysis continued, much larger quantities of charge were consumed and the solution eventually turned the deep blue color characteristic of highly reduced heteropolyanions. Analysis of the resulting solution revealed that significant quantities of NH_4^+ had been produced.

The efficiency of the catalytic electroreduction of nitrite to ammonia was examined by conducting a series of controlled-potential electrolyses under varying experimental conditions. With catalyst/nitrite ratios of unity or greater it was possible to reduce most of the nitrite present to ammonia with high faradaic efficiency. In one experiment the electrolysis was carried out in two stages: First the potential was maintained at −300 mV where the NO_2^- was converted quantitatively to the nitrosyl complex, $ONFe^{II}XW_{11}O_{39}^{(n+1)-}$. During this stage no ammonia could be detected in the solution. In the second stage the potential was adjusted to −900 mV, where the generation of ammonia commenced as the nitrosyl complex was reduced.

Experiments conducted under more realistic catalytic conditions, with catalyst-to-nitrite ratios much less than one, produced the results summarized in Table II. The quantity of charge consumed depended on the identity of the heteroatom present in the catalyst despite the very similar formal potentials of the processes corresponding to reduction of the tungsten–oxo framework for all of the catalysts.[1] The reasons for the variations in charge consumed are not clear although catalyzed hydrogen evolution by slow modification of the electrode surface as described by Nadjo and co-workers[9a-i] is one possibility. Analysis of the solutions at the point in the electrolysis where the first permanent blue color appeared (corresponding to an excess of multiply reduced catalyst) revealed the presence of substantial quantities of ammonia. The coulombic efficiencies with which the ammonia was generated are listed in Table II. It seems clear that both the identity of the central heteroatom and the ratio of catalyst to nitrite affect the amount of ammonia generated. We did not attempt to identify the other products of the catalyzed electroreduction quantitatively. However, the otherwise stable nitrosyl complexes of the heteropolytungstate catalysts, $ONFe^{II}XW_{11}O_{39}^{(n+1)-}$, were observed to react with excess NO_2^- to yield what appeared to be NO and oxidized catalyst. With the large excesses of NO_2^- present in the experiments of Table II, the NO generated in this way might well have escaped with the flowing argon from the unsealed reaction solution. (The aqueous solubility of NO is only 2 mM at 1 atm of pressure.[22]) This could account for the decrease in the quantity of ammonia generated as the ratio of nitrite to catalyst increased as well as for the disappearance of all of the nitrite upon the consumption of as little as 1.8 electrons per nitrite ion (experiment 6 in Table II).

Table II. Electrolytic Reduction of Nitrite to Ammonia As Catalyzed by Iron-Substituted Heteropolytungstates $Fe^{III}XW_{11}O_{39}^{n-}$ [a]

expt	X[b]	concn of cat.,[c] mM	sub/cat.[d]	electrons per NO_2^-[e]	redn to NH_3,[f] %	coul eff,[g] %
1	Si	0.47	40	3.6	21	35
2	Ge	0.45	41	7.7	29	22
3	P	0.46	43	6.4	31	49
4	As	0.44	40	3.8	36	35
5	P	0.47	84	2.6	13	29
6	P	0.10	368	1.8	10	33

[a] Supporting electrolyte: 0.1 M CH_3COONa–CH_3COOH, pH = 4. Stirred mercury pool maintained at −0.9 V. Except for experiment 5, electrolyses were halted at the first permanent appearance of the dark blue color characteristic of reduction of the tungsten–oxo framework of the catalysts. [b] Identity of the heteroatom in the catalysts. [c] Initial concentration of catalyst. [d] Ratio of substrate to catalyst. [e] The number of faradays of charge passed per mole of NO_2^- initially present. [f] Percent of the initial NO_2^- converted to NH_4^+ as determined by ion chromatography. [g] Coulombic efficiency for generation of ammonia: (moles of NH_4^+ per faraday of charge) × 6.

Nitrite might also be consumed without the consumption of faradaic charge via reaction 3.[17] Permanagnate titrations of

$$H^+ + 3HNO_2 \rightarrow NO_3^- + 2NO + 2H_2O \qquad (3)$$

solutions of NO_2^- in the supporting electrolytes employed showed that there was negligible loss on the time scale of typical electrolyses (~2 h). However, in the presence of the oxidized forms of the heteropolyanions, $H_2OFe^{III}XW_{11}O_{39}^{n-}$, some loss of NO_2^- occurred (ca. 10% in 2 h) and NO_3^- was detected in the solution. Thus the $H_2OFe^{III}XW_{11}O_{39}^{n-}$ anions may be mild catalysts for reaction 3.

The possibility that hydroxylamine is generated during the electrolysis was examined in experiment 5 of Table II by halting the electrolysis about halfway to completion where ca. 200 electrons per catalyst molecule had been consumed. Analysis of the electrolysis solution revealed the presence of only a small quantity of hydroxylamine (6.5×10^{-5} M) but a substantial quantity of ammonia. Since it was established in separate experiments that hydroxylamine is a much less reactive substrate than NO_2^- or NO, these results indicate that if hydroxylamine is formed during the catalyzed reduction of nitrite to ammonia, it is further reduced more rapidly than it can escape from the substrate–catalyst complex.

Discussion

The results described above have identified several steps in the chemistry that ensues when nitrite is exposed to the $H_2OFe^{II}XW_{11}O_{39}^{(n+1)-}$ complexes.

Formation and Reactivity of Nitrosyl Complexes. The formation of nitrosyl complexes by reaction of nitrite with complexes of Fe(II) is well-known[12,18] although the kinetics of the process have not been investigated extensively. The pH dependence of the cleanly second-order rate constant (k_{obsd}) for the formation of the complexes with heteropolytungstates as shown in Figure 4 is compatible with a mechanism in which $H_2OFe^{II}XW_{11}O_{39}^{(n+1)-}$ reduces HNO_2 to NO followed by the rapid coordination of NO by a second molecule of $H_2OFe^{II}XW_{11}O_{39}^{(n+1)-}$. Although the reduction step could, in principle, involve outer-sphere electron transfer, the alternative mechanism expressed in Scheme I, which

(22) *The Merck Index*, 9th ed.; Merck & Co.: Rahway, NJ, 1976; p 854.

Scheme I

$$NO_2^- + H^+ \overset{K_a}{\rightleftharpoons} HNO_2 \quad (4)$$

$$HNO_2 + H_2OFe^{II}XW_{11}O_{39}^{(n+1)-} \overset{K_5}{\rightleftharpoons} HNO_2Fe^{II}XW_{11}O_{39}^{(n+1)-} + H_2O \quad (5)$$

$$HNO_2Fe^{II}XW_{11}O_{39}^{(n+1)-} \xrightarrow{k_6} HOFe^{III}XW_{11}O_{39}^{(n+1)-} + NO \quad (6)$$

$$H_2OFe^{II}XW_{11}O_{39}^{(n+1)-} + NO \rightleftharpoons ONFe^{II}XW_{11}O_{39}^{(n+1)-} + H_2O \quad (7)$$

$$HOFe^{III}XW_{11}O_{39}^{(n+1)-} + H^+ \overset{K_8}{\rightleftharpoons} H_2O\ Fe^{III}XW_{11}O_{39}^{n-} \quad (8)$$

features an inner-sphere electron-transfer step, seems preferable. Reactions 4 and 5 are fast preequilibria, reaction 6 is the rate-determining step, and rections 7 and 8 are fast follow-up steps. There are several reasons that we prefer Scheme I over the corresponding outer-sphere pathway: (i) The strongly reducing lacunary anions, $XW_{11}O_{39}^{(n+3)-}$, which lack a suitable coordination site for HNO_2 (or NO_2^-), do not reduce HNO_2 (or NO_2^-) at an appreciable rate despite their much more negative formal potentials (Figure 2D). (ii) Assuming that the equilibrium constant for reaction 5 is not large, the driving force for reaction 6 is considerably greater than that of the corresponding outer-sphere reaction (which would yield uncoordinated hydroxide ion) because of the affinity of the iron(III) center for hydroxide ion. For example, in the case of X = Si the driving force advantage for the inner-sphere pathways amounts to ca. 450 mV because K_8 is only 2×10^6 M^{-1}.[1] (iii) Voltammograms of equimolar mixtures of NO_2^- and $H_2OFe^{III}XW_{11}O_{39}^{n-}$ at pH 5 or above show no evidence of a catalytically enhanced reduction at potentials corresponding to the Fe^{III}/Fe^{II} couple (Figure 2B). This behavior is in accord with the rate constants listed in Table I for the formation of the nitrosyl complexes which correspond to negligible formation of the complexes during the time required to record the voltammograms in Figure 2C. However, at the more negative potentials where reduction of the tungsten–oxo framework occurs, significant catalytic currents are observed (Figure 2C). Coordination of NO to the reduced iron center has been shown to be a prerequisite for its catalytic reduction so that a faster route to the nitrosyl complex must be available to account for the observed catalysis. That faster route seems most likely to be the reduction of the coordinated HNO_2 in the $HNO_2Fe^{II}XW_{11}O_{39}^{(n+1)-}$ complex formed in equilibrium 5 of Scheme I, not by electrons originating in the Fe(II) center as in eq 6, but by the much more energetic electrons available at electrode potentials in the range where the tungsten–oxo framework of the complex is reduced. (The possibility that the HNO_2 might be activated by coordination and become directly reducible at the electrode at the more negative potentials seems remote because there is little reason for such a direct reduction to follow so closely the variations in the potentials where the tungsten–oxo framework is reduced as the central heteroatom is changed.) Thus the voltammetry of Figure 2C, which cannot be reconciled with an outer-sphere mechanism for the reduction of HNO_2, can be nicely accommodated by Scheme I.

Attempts to measure spectroscopically the rate of reaction 7 in the forward direction by manually mixing NO with the reduced complex were thwarted by the high rate of the reaction. Reaction 7 is written as reversible because the nitrosyl complex is eventually converted to the original aquo complex when NO is removed from solutions of the complex by extensive bubbling with argon. The observation that the $ONFe^{II}XW_{11}O_{39}^{(n+1)-}$ complexes react with excess NO_2^- can be understood as taking place through the inverse of reaction 7 followed by reaction 5. The possibility that the NO involved in reaction 7 is generated via reaction 3 instead of reaction 6 could be eliminated because the rate of reaction 3 is too low.[17] The apparent preference for HNO_2 over NO_2^- as the oxidant in reaction 6 is not surprising because it avoids the generation of the high-energy O^{2-} anion.

Table III. Correlation between the First Reduction Potentials of the Tungsten–Oxo Framework and the Potential Where $Fe^{III}XW_{11}O_{39}^{n-}$ Complexes Catalyze the Reduction of NO[a]

X[b]	$-E^f$,[c] mV	$-E_{cat}$,[d] mV
Si	752	760
Ge	725	730
P	702	730
As	690	710

[a] $[Fe^{III}XW_{11}O_{39}^{n-}] = [NO_2^-] = 1$ mM; supporting electrolyte: 0.1 M CH_3COONa–CH_3COOH, pH = 4. Scan rate = 50 mV/s. [b] Identity of central heteroatom. [c] Formal potential of the $Fe^{II}XW_{11}O_{39}^{(n+1)-}/Fe^{II}XW_{11}O_{39}^{(n+3)-}$ couple. [d] Potential where the current in the presence of NO is 5% larger than the current in its absence.

The values of k_{obsd} measured at pH 5 are listed in Table I. The reaction rate responds to changes in the reducing strength of the heteropolyanion produced by changing the central heteroatom. The stronger reductants appear somewhat more reactive. However, according to Scheme I, the measured values of k_{osbd} correspond to the product $K_5k_6([H^+]/(K_a + [H^+]))$, where K_5 and k_6 are the equilibrium constant and rate constant for reactions 5 and 6, respectively, and K_A is the acid dissociation constant of HNO_2. (At pH 5, $k_{obsd} = 2 \times 10^{-2}\ K_5k_6$). It was not possible to measure K_5 independently so it remains unclear whether the trend in k_{obsd} evident in Table I reflects an increase of k_6 or K_5 (or both) with the reducing strength of the heteropolyanion.

Electrochemistry of the $ONFe^{II}XW_{11}O_{39}^{(n+1)-}$ Complexes. The peak current for the first, new, irreversible, anodic wave obtained in voltammograms for the nitrosyl complexes (Figure 5, curve C) corresponds to more than one electron. The position of the wave shifts as the identity of the heteroatom is changed in the same way as does the formal potential of the Fe^{III}/Fe^{II} couple in the parent heteropolytungstate. This behavior is consistent with the interpretation of the wave as an essentially iron-based electrode reaction, i.e., the oxidation of Fe(II) to Fe(III) which induces the release and subsequent oxidation of the nitrosyl ligand. The $H_2OFe^{III}XW_{11}O_{39}^{n-}$ ions exhibit no affinity for NO so that its dissociation from the oxidized complex is to be expected and free NO is known to be electrooxidized at the potentials where the first anodic wave appears.[23] Thus the wave is reasonably assignable to the half-reaction specified in eq 9. The irreversibility

$$ONFe^{II}XW_{11}O_{39}^{(n+1)-} - 2e^- + 2H_2O \rightarrow NO_2^- + H_2OFe^{III}XW_{11}O_{39}^{n-} + 2H^+ \quad (9)$$

of the first anodic wave is the result of the large positive shift in the potential where the Fe(II) center is oxidized when it is coordinated to NO. The $H_2OFe^{III}XW_{11}O_{39}^{n-}$ anion generated during the anodic oxidation is reducible only at much more negative potentials. The large positive shift in the potential where the oxidation of Fe(II) occurs in the $ONFe^{II}XW_{11}O_{39}^{(n+1)-}$ complexes is consistent with substantial back-donation of electrons by the Fe(II) center into a π^* orbital of the coordinated NO as was invoked earlier to account for the correlation between the position of the infrared absorption of the coordinated NO and the reducing power of the Fe(II) center (Table I).

The second anodic wave in curve D of Figure 5 appears at the same potential for all four heteropolyanions and corresponds to the potential where NO_2^- is irreversibly oxidized to NO_3^- in separate experiments. The same wave appears whether the nitrosyl complex is prepared by reacting the parent Fe(II) complex with NO_2^- or with NO so that it is clearly associated with the nitrosyl complex itself and not with any residual, unreacted NO_2^- in solution.

Reduction of Coordinated NO. The potential where the catalyzed reduction of the coordinated NO commences in curve E of Figure 5 corresponds to the potential of the first, two-electron reduction of the tungsten–oxo framework in the catalyst. The correlation between the two sets of potentials is evident from the

(23) Cutta, D.; Landolt, D. *J. Electrochem. Soc.* **1972**, *119*, 1320.

values listed in Table III. The potentials of the Fe^{III}/Fe^{II} couples for both the aquo and nitrosyl complexes also shift with the identity of the heteroatom (Table I) but this shift does not correlate as closely with the potentials where the catalyzed reductions of the coordinated NO proceed (Table III). These observations constitute strong circumstantial evidence that the electrons accepted by the NO group that is bound to the Fe(II) center are delivered via the tungsten–oxo framework and not directly from the electrode. The implication is that the tungsten cage serves as a reservoir for the storage of electrons that are subsequently transferred to the NO group in a concerted, intramolecular, multiple-electron process that is more facile than direct reduction at the electrode. Note that this assertion would be much more difficult to make with confidence were it not for the observed systematic shifts in potential as the identity of the central heteroatom was changed. The ability of the $FeXW_{11}O_{39}^{n-}$ anions to serve as both the site of substrate binding and the source of the reducing electrons evidently contributes to the unique catalytic reactivity patterns that they display. The reason that the electrons that reduce the coordinated NO follow the circuitous route that leads from the electrode to the tungsten–oxo framework and to the iron(II) center before reaching the NO molecule that is the object of their journey may be understood as the result of the back-bonding between the NO and the Fe(II). Unoccupied orbitals on the NO that can accept electrons from the electrode before its coordination to Fe(II) are apparently partially occupied after the coordination, and the multiple, empty orbitals available within the tungsten–oxo framework are evidently the most accessible point of entry to the complex for electrons from the electrode.

Catalyst Durability. To examine the robustness of the catalysts toward repeated cycling under realistic electrolytic conditions, a series of electrolyses were carried out in single-compartment cells without separation of the anode and cathode. Large excesses of NO_2^- were added to 0.5 mM solutions of the catalysts. Under these conditions the NO_2^- was consumed both by reaction with the reduced heteropolytungstate generated at the mercury cathode and by oxidation to nitrate at the platinum anode. Presumably the anodic oxidation proceeded both by direct oxidation of NO_2^- and by oxidation of the $ONFe^{II}XW_{11}O_{39}^{(n+1)-}$ nitrosyl complex whose generation at the cathode (vide supra) was evident from the red color of the solution. Electrolyses were continued until the dark blue color characteristic of the multiply reduced catalysts persisted in the solution to indicate the complete consumption of NO_2^- by reduction and oxidation. At this point, any change in the catalyst concentration was estimated by comparing cyclic voltammetric peak heights with those measured before the electrolyses. No loss of catalyst was detected after 100 electrons per catalyst molecule had been passed, and even with 900 electrons per molecule the loss did not exceed 5% and there was no cyclic voltammetric evidence that new electroactive species had been generated by the repeated cycling. Thus, our initial hope that the entirely inorganic heteropolytungstates would prove to be extremely resistant to oxidative and reductive degradation was realized.

Comparison with the Behavior of Other Catalysts for Nitrite Reduction. The redox chemistry and electrochemistry exhibited by the $H_2OFe^{III}XW_{11}O_{39}^{n-}$ catalysts in the presence of NO_2^- and NO contrasts with that described recently for water-soluble iron porphyrins[12] and nickel and cobalt cyclam complexes[13] that serve as catalysts for the reduction of NO_2^- and NO and with the behavior of ruthenium and osmium polypyridyl complexes that facilitate stoichiometric reductions of NO_2^- and NO.[14] The iron and nickel cyclam catalysts operate at significantly more negative potentials (−1.5 V) than the $H_2OFe^{III}XW_{11}O_{39}^{n-}$ catalysts and the iron porphyrin catalysts yield a different set of reduction products. For example, while hydroxylamine (or its dehydrated equivalent) was found to be a significant side product or an active intermediate in most previous catalytic studies,[11-14] the $H_2OFe^{III}SiW_{11}O_{39}^{5-}$ catalysts produced only traces of hydroxylamine even when the electrolyses were stopped near their midpoints where intermediates might have been expected to accumulate. The possibility that the heteropolyanion might also catalyze the reduction of hydroxylamine was ruled out by adding a tenfold excess of hydroxylamine to a 1 mM solution of the catalyst and noting no change in the cyclic voltammetry of the catalyst. Hydroxylamine was also shown to be stable in solutions of the supporting electrolytes and catalysts over time scales comparable to those involved in the electrolyses (~2 h).

The redox potentials for the Fe^{III}/Fe^{II} couples in the porphyrins are similar to those in the iron-substituted heteropolytungstates but the two types of complexes behave differently toward NO and NO_2^-. The Fe(III) forms of the porphyrins react with NO to form a nitrosyl complex that can be reduced in two one-electron steps.[12a] In the presence of excess NO_2^- and protons the iron(III) porphyrins are converted to the same reducible nitrosyl complex by reactions with the NO generated by the disproportionation of HNO_2.[12a] By contrast, the $H_2OFe^{III}XW_{11}O_{39}^{n-}$ complexes are unreactive toward both NO and NO_2^-.

The iron(II) forms of the porphyrins react with an excess of NO_2^- in neutral solutions to yield a reduced form of the nitrosyl complex according to unspecified stoichiometry.[12] Here the $H_2OFe^{II}XW_{11}O_{39}^{(n+1)-}$ complexes behave similarly and exhibit the clean stoichiometry ($2Fe^{II}$ per NO_2^-) expressed in eq 5 and 7 of Scheme I.

The nitrosyl complexes of the iron porphyrins can apparently exist in three quasi-stable oxidation states separated by one electron and with formal potentials positive of those where the catalytic, dissociative reduction of the nitrosyl ligand proceeds.[12] These oxidation states have been depicted as representing iron(II) complexes of NO^+, NO^0, and NO^-. There is no analogous set of stable oxidation states for the $ONFe^{II}XW_{11}O_{39}^{(n+1)-}$ complexes. Oxidation of these complexes leads to dissociation (and subsequent oxidation) of the nitrosyl ligand (Figure 5C–D), and their first observable reduction, which occurs at potentials where the tungsten–oxo framework is reduced, results in their destruction with the generation of ammonia (and possibly other reduction products) (Figure 5E). In contrast with the iron porphyrins, no ammonia is detected when bulk electrolyses are performed at potentials just negative to the Fe^{III}/Fe^{II} couple.

The greater stability and more extensive set of stable oxidation states for the nitrosyl complexes of the iron porphyrins compared with the iron-substituted heteropolytungstates doubtless reflect the more extensive back-bonding that occurs with the former complexes. The difference in back-bonding ability of the Fe(II) centers between the two classes of complexes can also be demonstrated by the relative reactivity toward CO. The $H_2OFe^{II}XW_{11}O_{39}^{(n+1)-}$ complexes show no tendency to bind CO[24] while Fe(II) porphyrins are well-known to do so. The same factor is likely to be the origin of the differences in the pattern of reactivity exhibited by the two classes of complexes during the catalytic reduction of the nitrosyl ligand to lower oxidation states. With the porphyrin complexes the reducing electrons appear to be added directly to the coordinated nitrosyl ligand with little, if any, participation by other reducible groups such as the methylpyridinium substituents in the iron *meso*-tetrakis(*N*-methyl-4-pyridyl)porphyrin.[12b] One result is a variety of intermediate reduction products, including hydroxylamine.[12] By contrast, the nitrosyl complexes of the iron-substituted heteropolytungstates appear to utilize the reducible tungsten–oxo core to store the reducing electrons temporarily before they are delivered to the unreduced, coordinated nitrosyl ligand in a concerted fashion. Thus, the differences between porphyrins and lacunary heteropolytungstates as ligands for iron(II) lead to significant differences in the outcome of electroreductions in which they are employed as catalysts.

In biological systems the six-electron reduction of nitrite to ammonia is accomplished by the nitrite reductase enzymes.[25] It has been demonstrated that the active site in these enzymes is an iron chlorin.[26] It has also been observed that there is a separate

(24) Toth, J. E.; Anson, F. C., unpublished experiments.
(25) Losada, M. *J. Mol. Catal.* **1975**, *1*, 245.
(26) Murphy, M. J.; Siegel, L. M.; Tove, S. R.; Kamin, M. *Proc. Natl. Acad. Sci. U.S.A.* **1974**, *71*, 612.

iron-sulfur center present in these enzymes[27] and that electron transfer occurs between the two iron sites.[25] It has been recently suggested[12b] that the iron-sulfur center may act as an electron reservoir which can deliver electrons to the iron chlorin active site to facilitate the multiple-electon reduction of bound nitrite. The $H_2OFe^{II}XW_{11}O_{39}^{(n+1)-}$ complexes behave in a similar fashion, with the tungsten-oxo framework acting like the iron-sulfur electron reservoir and the coordinated iron center acting like the active iron chlorin site in the enzyme. Thus, in a number of respects, the iron-substituted heteropolytungstates act as totally inorganic enzyme mimics.

(27) Aparicio, P. J.; Knaff, D. B.; Malkin, R. *Arch. Biochem. Biophys.* **1975**, *169*, 102.

Concluding Remarks

The electrocatalytic chemistry we have described for the iron-substituted heteropolytungstates in solutions of nitrite and nitric oxide represents the first example of a durable, entirely inorganic electrocatalyst that exhibits both binding of a substrate and subsequent multiple-electron reduction. The unique pattern of catalytic activity displayed by these transition-metal-substituted heteropolyanions, especially their ability to store and deliver multiple electrons to a bound substrate, seems likely to be useful in additional contexts that are the subjects of continuing investigations.

Acknowledgment. This work was supported by the National Science Foundation.

Effects of Solvent and Anomeric Configuration upon the Circular Dichroism, Temperature Dependence of Amide Proton Chemical Shifts, Amide Proton Exchange Rates, and Infrared Absorption of Methyl 2-Acetamido-2-deoxy-D-glucopyranosides

L. A. Buffington,* D. W. Blackburn, C. L. Hamilton, T. C. Jarvis, J. J. Knowles, P. A. Lodwick, L. M. McAllister, D. J. Neidhart, and J. L. Serumgard

Contribution from the Department of Chemistry, Carleton College, Northfield, Minnesota 55057.
Received August 17, 1987

Abstract: Explanations were sought for the dependence upon anomeric configuration of the temperature dependence of the NMR chemical shifts of amide protons, $\Delta\delta/\Delta T$, in 2-acetamido-2-deoxy-D-glucopyranosides. Measurements in several solvents were made of $\Delta\delta/\Delta T$, of amide circular dichroism, of amide infrared absorption frequencies, and of rates of exchange of amide protons with solvent protons. The effect of solvent upon the relative $\Delta\delta/\Delta T$ values of the two anomers varies and correlates with the effect of solvent upon the relative molar ellipticities of the two anomers. The α amide I frequencies and the α rates of exchange with solvent, however, are less than those of the β anomer in all solvents studied. The "normal" (for peptide conformational analyses) correlation between high $|\Delta\delta/\Delta T|$ values and high solvent exchange rates is not observed. It is suggested that the "conventional" interpretation of high $|\Delta\delta/\Delta T|$ values in terms of solvent exposure does not apply and, more tentatively, that the two anomers differ in intramolecular hydrogen bonding.

The temperature dependence, $\Delta\delta/\Delta T$, of the NMR[1] chemical shifts of the exchangeable protons of biomolecules is often used in conformational studies as an indicator of exposure of the proton to the solvent. The most widely used interpretation of $\Delta\delta/\Delta T$ values is that a relatively large dependence upon temperature means that the proton is relatively exposed to the solvent while a lesser dependence upon temperature suggests that the proton is involved in a hydrogen bond or is otherwise sequestered from the solvent. This interpretation was established through the measurement of $\Delta\delta/\Delta T$ values in peptides of known conformation and has been applied to amide protons in peptides[2] and carbohydrates[3] and to hydroxyl protons in carbohydrates.[3,4] The association of high $|\Delta\delta/\Delta T|$ values with solvent exposure can be rationalized as follows: A solvent-exposed proton is likely to hydrogen bond with the solvent and as the temperature is increased this hydrogen bonding is disrupted, decreasing the chemical shift. It has been recognized, however, that exchangeable protons that are not solvent exposed can exhibit high $|\Delta\delta/\Delta T|$ values if they are involved in other temperature-dependent interactions, especially in nonpolar solvents.[3,5]

We previously reported that, for some sugars in DMSO and water, the $|\Delta\delta/\Delta T|$ values of exchangeable protons of carbon 2 (Figure 1) substituents were greater for α anomers than for β anomers.[6] Here we focus on a pair of anomeric glucopyranosides and report that the dependence upon anomeric configuration is solvent dependent. We also use CD, hydrogen to deuterium exchange rates, and IR absorption to seek an understanding of the factors affecting the $\Delta\delta/\Delta T$ values. The importance of such an understanding is manyfold. It should help to (1) determine how $\Delta\delta/\Delta T$ values should be used in conformational studies of carbohydrates, (2) learn more about the conformational properties

(1) Abbreviations used: NMR, nuclear magnetic resonance; DMSO, dimethyl sulfoxide; CD, circular dichroism; IR, infrared; UV, ultraviolet; α, methyl 2-acetamido-2-deoxy-α-D-glucopyranoside; β, methyl 2-acetamido-2-deoxy-β-D-glucopyranoside; HFIP, hexafluoroisopropyl alcohol; HFB, heptafluorobutanol; TFE, trifluoroethanol; TMS, trimethylsilane; DMF, dimethylformamide.

(2) (a) Llinas, M.; Klein, M. P. *J. Am. Chem. Soc.* **1975**, *97*, 4731-4737, and references therein. More recent examples are: (b) Kessler, H.; Bernd, M.; Kogler, H.; Zarbock, J.; Sorensen, O. W.; Bodenhausen, G.; Ernst, R. R. *J. Am. Chem. Soc.* **1983**, *105*, 6944-6958. (c) Pope, M.; Mascagni, P.; Gibbons, W. A.; Ciufetti, L. M.; Knoche, L. M. *J. Am. Chem. Soc.* **1984**, *106*, 3863-3864. (d) Kartha, G.; Bhandary, K. K.; Kopple, K.; Go, A.; Zhu, P. *J. Am. Chem. Soc.* **1984**, *106*, 3844-3850.

(3) Heatley, F.; Scott, J. E.; Jeanloz, R. W.; Walker-Nasir, E. *Carbohydr. Res.* **1982**, *99*, 1-11, and references therein.

(4) St.-Jacques, M.; Sundararajan, P. R.; Taylor, K. J.; Marchessault, R. H. *J. Am. Chem. Soc.* **1976**, *98*, 4386-4391.

(5) (a) Stevens, E. S.; Sugarawara, N.; Bonora, G. M.; Toniolo, C. *J. Am. Chem. Soc.* **1980**, *102*, 7048-7050. (b) Pease, L. G.; Watson, C. *J. Am. Chem. Soc.* **1978**, *100*, 1279-1286.

(6) Buffington, L.; Crusius, J.; Nachbor, M.; Reven, L. *J. Am. Chem. Soc.* **1983**, *105*, 6745-6747.

0002-7863/89/1511-2451$01.50/0